MONTE CARLO AND MOLECULAR DYNAMICS SIMULATION OF URANYL ADSORPTION ON MONTMORILLONITE CLAY

OMAR F. ZAIDAN[1], JEFFERY A. GREATHOUSE[1,*] AND ROBERTO T. PABALAN[2]

[1] Department of Chemistry, St. Lawrence University, Canton, NY 13617, USA
[2] Center for Nuclear Waste Regulatory Analyses, Southwest Research Institute, 6220 Culebra Road, San Antonio, TX 78238, USA

Abstract—We performed Monte Carlo and molecular dynamics simulations to investigate the interlayer structure of a uranyl-substituted smectite clay. Our clay model is a dioctahedral montmorillonite with negative charge sites in the octahedral sheet only. We simulated a wide range of interlayer water content (0 mg H_2O/g clay – 260 mg H_2O/g clay), but we were particularly interested in the two-layer hydrate that has been the focus of recent X-ray absorption experiments. Our simulation results for the two-layer hydrate of uranyl-montmorillonite yield a water content of 160 mg H_2O/g clay and a layer spacing of 14.66 Å. Except at extremely low water content, uranyl cations are oriented nearly parallel to the surface normal in an outer-sphere complex. The first coordination shell consists of five water molecules with an average U–O distance of 2.45 Å, in good agreement with experimental data. At low water content, the cations can assume a perpendicular orientation to include surface oxygen atoms in the first coordination shell. Our molecular dynamics results show that $UO_2(H_2O)_5^{2+}$ complexes translate within the clay pore through a jump diffusion process, and that first-shell water molecules are exchangeable and interchangeable.

Key Words—Computer Simulation, Molecular Dynamics, Monte Carlo, Montmorillonite, Uranyl.

INTRODUCTION

An important consideration in safety assessments of nuclear waste repositories and in nuclear waste management is the migration of radionuclides to the accessible environment. Radionuclide transport in the subsurface can be mitigated by sorption interactions with minerals along groundwater flow paths. Clay minerals are ubiquitous components of rocks, soils and sediments, and sorption interaction with these minerals can retard radionuclide migration in many geochemical environments. In addition, some proposed nuclear waste repositories plan to emplace compacted bentonite material, composed mainly of montmorillonite, between the nuclear waste containers and the surrounding rocks to serve as an engineered barrier that would limit the movement of radionuclides from the repository (Grauer, 1994; Lajudie *et al.*, 1994; Neall *et al.*, 1995).

In this study, we used molecular simulations to study the sorption of U on the clay mineral montmorillonite. Uranium is the predominant heavy metal in spent nuclear fuel (>95% UO_2) and is a major contaminant in the soils, subsurface, or groundwaters of many sites in the US due to mining and milling of uranium ores and to production of nuclear weapons (Riley *et al.*, 1992; National Research Council, 2000). Uranium occurs in the 6+ oxidation state under near-surface conditions and its various aqueous species, predominantly the aquo-,

hydroxy- and carbonato-complexes, make it potentially very mobile in the environment. Sorption experiments have shown that U(6+) can sorb onto montmorillonite through two distinct mechanisms – ion exchange with interlayer cations and surface complex formation with hydroxylated edge sites (*e.g.* Zachara and McKinley, 1993; McKinley *et al.*, 1995; Pabalan and Turner, 1997; Hyun *et al.*, 2001; Chisholm-Brause *et al.*, 2001). These mechanisms arise from the distinct mineralogic character of montmorillonite, which is a smectite clay with an expandable 2:1 layered structure, characterized by a plane of octahedrally coordinated Al atoms sandwiched between two planes of tetrahedrally coordinated Si atoms. Substitution of Mg^{2+} or Fe^{2+} for Al^{3+} in the octahedral sites, or of Al^{3+} for Si^{4+} in the tetrahedral sites, results in a net negative charge that is balanced by interlayer cations. These cations are hydrated and readily exchanged, for example with the uranyl cation, UO_2^{2+}. In addition, the edge surfaces of montmorillonite particles provide surface hydroxyl sites for sorption of radionuclide species. Uranium sorption at these amphoteric edge sites is analogous to sorption on the surface of oxides such as quartz, alumina and ferrihydrite (McKinley *et al.*, 1995; Sylwester *et al.*, 2000; Greathouse *et al.*, 2002).

The relative importance of the two sorption mechanisms depends on solution chemistry. Uranyl sorption onto negatively charged cation-exchange sites is favored when the aqueous solution has low pH and low concentration of competing cations (Hyun *et al.*, 2001). Uranyl sorption onto the amphoteric edge sites is

* E-mail address of corresponding author:
jgreathouse@stlawu.edu

favored in the pH range where uranyl hydroxy-complexes are the predominant aqueous species (Pabalan *et al.*, 1998). Thus, under ambient pCO_2 conditions, uranyl sorption on the edge sites is highest at near-neutral pHs and decreases towards more acidic conditions, where the uranyl aquo species is predominant, or more alkaline conditions, where uranyl-carbonate complexes are major species (Pabalan and Turner, 1997).

Published studies using X-ray absorption spectroscopy (XAS), which includes X-ray absorption near-edge structure (XANES) and extended X-ray absorption fine structure (EXAFS) spectroscopy, show that U sorbed on montmorillonite remains in the 6+ oxidation state as the linear UO_2^{2+} moiety (Dent *et al.*, 1992; Sylwester *et al.*, 2000; Reeder *et al.*, 2001). However, the equatorial coordination of uranyl, *i.e.* the number and arrangement of atoms coordinated along the equatorial plane of the linear uranyl ion, is different under conditions that favor sorption at ion-exchange sites *vs.* hydroxylated edge sites. The EXAFS results show that the structure of U sorbed from solutions of low pH (~3 to 4) and low ionic strength, conditions that favor sorption on ion-exchange sites, exhibits a uniform equatorial shell of oxygen ligands, with a coordination number of 5±1 and a $U-O_{eq}$ distance of ~2.4 Å, similar to that of the free uranyl pentaaquo species (Dent *et al.*, 1992; Sylwester *et al.*, 2000; Reeder *et al.*, 2001). In contrast, the structure of U sorbed from solutions at near-neutral pH (~6.4), which favor sorption on hydroxylated edge sites, shows a pronounced splitting into two equatorial shells, with $U-O_{eq}$ distances of ~2.3 and ~2.5 Å and a total coordination number ranging from 4 to 6 (Sylwester *et al.*, 2000; Reeder *et al.*, 2001). The EXAFS does not determine directly if the coordinating oxygen atom is contributed by a solvating water, by a hydroxide or carbonate ligand, or by a surface hydroxyl group. Nevertheless, the fairly symmetric equatorial shell for U sorbed at low pH is considered evidence for formation of an outer-sphere complex at cation-exchange sites, whereas the equatorial splitting observed in the structure of uranyl sorbed at near-neutral pH is considered the result of inner-sphere complexation of the uranyl ion with hydroxylated edge sites (Sylwester *et al.*, 2000). In addition, a recent polarized XAS study indicated that the UO_2^{2+} cations in the interlayer ion-exchange sites of montmorillonite have an orientation that is neither perpendicular nor parallel to the basal planes (Denecke *et al.*, 1999), rather, the OUO^{2+} molecular axis is tilted at an angle relative to the surface normal.

Molecular simulations of U sorption were conducted in this study to provide information that complements that derived from sorption experiments and XAS studies. Using computer simulation techniques, one can explore the structure and dynamics of many-body systems, particularly systems with one or more interfaces. Additionally, the use of three-dimensional periodic boundary conditions commonly used in such simulations lends itself nicely to smectite hydrates, which comprise alternating layers of clay mineral and aqueous interlayer phases. Computer simulation of the clay-water interface has become an active area of research. While most published studies treat the clay structure as a rigid body, a few groups have used a flexible clay model (Teppen *et al.*, 1997; Hartzell *et al.*, 1998). An examination of the effects of clay hydroxyl orientation is possible with a flexible-atom model. Additionally, the presence of charge sites in the tetrahedral sheet warrant the use of a flexible-atom model as surface relaxation is more likely to occur in this case than with octahedral substitution. Our clay model used in this study contains only octahedral charge sites, so we are confident in our use of a rigid-body approach. The complexity of interlayer species studied has grown from monatomic cations (Skipper *et al.*, 1991; Chang *et al.*, 1995; Chang *et al.*, 1997; Smith, 1998; Chang *et al.*, 1998; Young and Smith, 2000; Greathouse *et al.*, 2000; Chavez-Paez *et al.*, 2001) to polyatomics (Hartzell *et al.*, 1998; Teppen *et al.*, 1998).

Greathouse *et al.* (2002) reviewed recent theoretical studies of UO_2^{2+}. Here we present results for the first simulations of a uranyl-substituted smectite clay. The goal of this research is to provide a detailed view of uranyl-montmorillonite surface complexes, but the study presented in this paper is focused on the interlayer region, including equilibrium interlayer structure and mobility of uranyl complexes. After detailing our Monte Carlo (MC) and molecular dynamics (MD) simulation methods, we first present results for the equilibrium structure (MC). We then present MD results, which provide the time evolution of interlayer properties.

SIMULATION METHODS

System configuration and parameters

All species were treated as rigid bodies. The montmorillonite model used in this study is based on previous models (Skipper *et al.*, 1991, 1995), except that charge substitution was introduced exclusively in the octahedral sheet (Mg^{2+} for Al^{3+}). We therefore avoided difficulties associated with tetrahedral charge, such as degree of charge delocalization, incorrect ion exchange free energy prediction (Young and Smith, 2000), and surface relaxation (Teppen *et al.*, 1997). We are confident that a rigid clay structure will produce reliable simulation results because the degree of surface relaxation should be minimal when no tetrahedral charge sites are present. Additionally, our choice for all-octahedral charge substitution allows for direct comparison with recent EXAFS experiments of uranyl-smectite complexes, in which SAz-1 clay was used (Sylwester *et al.*, 2000; Reeder *et al.*, 2001). SAz-1 has the unit-cell formula $M_{1.2}^{+}[Si_8](Al_{2.67}Fe_{0.15}Mg_{1.20})O_{20}(OH)_4$ (Breen *et al.*, 1995). The repeating supercell consisted of eight unit-

cells of montmorillonite, with octahedral cations located at $z = 0$. We created negative charge sites by replacing 6 Al^{3+} cations in the octahedral sheet with Mg^{2+} cations. Potential parameters are based on pairwise interactions and include electrostatic and van der Waals terms as follows:

$$U_{ij} = \frac{q_i q_j}{r} + \frac{A_i A_j}{r^{12}} - \frac{B_i B_j}{r^6} \qquad (1)$$

In equation 1, U_{ij} is the potential energy (in kJ mol^{-1}) between atoms i and j separated by a distance r (in Å), q_i is the charge of atom i, and the A_i and B_i are van der Waals parameters for atom i. We used the three-site SPC/E water model (Berendsen *et al.*, 1987) which has been used successfully in previous ion-clay simulation studies (Young and Smith, 2000). In the SPC/E model, van der Waals interactions between water molecules occur between oxygen atoms only. For water-clay interactions, we followed the method of Skipper *et al.* (1995), by including van der Waals interactions between water oxygen atoms and surface oxygen atoms. For uranyl-water interactions, we used a model developed for aqueous uranyl complexes (Guilbaud and Wipff, 1996), which has produced first-shell U−O distances and hydration free energies in good agreement with experimental results. For rigid-body simulations such as ours, we ignore the intramolecular terms (angle bending and bond stretching). However, we have performed simulations of the rigid uranyl model in bulk solution, resulting in identical uranyl-water radial distribution results as the flexible model (data not shown) (Guilbaud and Wipff, 1996). Uranyl-clay interactions include van der Waals terms between uranyl U atoms and surface oxygen atoms and between uranyl oxygen atoms and surface oxygen atoms. All potential parameters are listed in Table 1. For all simulations, three-dimensional periodic boundary conditions were used to produce a repeating macroscopic system, and the Ewald sum technique (Allen and Tildesley, 1987) was used for electrostatic interactions. For van der Waals interactions, a real-space cutoff of 9.0 Å was imposed.

Monte Carlo simulations

The program MONTE v. 3.2 (Skipper, 1996) was run on single-processor workstations (Silicon Graphics O2 and Octane) and a Silicon Graphics Origin 300 super-computer. We used the constant ($N\sigma T$) ensemble, with temperature (T) and pressure (σ) values fixed at 300 K and 100 kPa, respectively, and N representing the number of interlayer water molecules. Strictly speaking, N should refer to the total number of particles in the simulation supercell, but we use it here to represent the number of interlayer water molecules as the clay composition remains fixed. The supercell was constructed with an initial layer spacing at least 2.0 Å greater than the anticipated equilibrium value. Throughout the simulation, the **a** and **b** supercell vector components had fixed values of $a_x = 21.12$ Å, $b_y = 18.28$ Å, and $a_y = a_z = b_x = b_z = 0$. The supercell **c** vector represents the location of the upper clay layer relative to the lower clay layer, with c_z representing the layer spacing and $c_x = c_y = 0$ initially. Registration is thus represented by c_x and c_y and refers to the lateral movement of one clay layer with respect to the adjacent layer. The interlayer region consisted of N water molecules and three uranyl ions placed randomly in the interlayer region, with U atoms residing at the midplane ($c_z/2$). The equilibration process followed the standard procedure (Greathouse and Storm, 2002). The first two stages consisted of 100,000 steps each, with allowed movement of interlayer molecules only (Stage 1), then movement of interlayer molecules and c_z (Stage 2). Two or more pre-equilibrium stages followed in which all motion was allowed (interlayer molecules, c_x, c_y, c_z). Equilibrium was established by monitoring the convergence of potential energy and layer spacing values. After that point, data were collected and averaged over a final stage of at least 500,000 steps. Density profiles and radial distribution functions (RDFs) were created by a continuous binning process within the MONTE code. Both water oxygen atoms and clay oxygen atoms were included in the U−O RDFs. Coordination numbers were obtained by integrating each RDF peak up to its minimum value (Floris *et al.*, 1994).

Table 1. Potential parameters as defined by equation 1.

Layer	Atom type (i)	q_i (e)	A_i (kJ mol^{-1} Å^{12})$^{1/2}$	B_i (kJ mol^{-1} Å^{6})$^{1/2}$
Interlayer	O (uranyl)	−0.250	1622.78	51.16
	U (uranyl)	2.500	1288.10	56.74
	O (water)	−0.848	1622.78	51.16
	H (water)	0.424	0.00	0.00
Tetrahedral	O	−0.800	1622.78	51.16
	Si	1.200	0.00	0.00
Apical	O	−1.000	0.00	0.00
Octahedral	O	−1.424	0.00	0.00
	H	0.424	0.00	0.00
	Al	3.000	0.00	0.00
	Mg	2.000	0.00	0.00

Molecular dynamics simulations

The program MOLDY v. 2.16 (Refson, 2000) was used in a constant (NVT) ensemble, where V represents the supercell volume, and run on a Silicon Graphics Origin 300 supercomputer. An equilibrated MC configuration was used as the starting point, and initial velocities were assigned according to a Boltzmann distribution. Because the c_x, c_y and c_z values are held fixed during an (NVT) simulation, the initial configuration was chosen with a layer spacing within 0.1 Å of the MC average. Temperature was maintained at 300 K with a Nosé-Hoover thermostat (Allen and Tildesley, 1987; Refson, 2000), with separate scaling for each molecular species. We used a 0.0005 ps timestep for all MD simulations. Following an equilibration period of 10 ps, data were collected for an additional 1000 ps (1 ns).

RESULTS AND DISCUSSION

Structural properties

In order to investigate the swelling behavior of this model system, a series of MC simulations were carried out with a range of water content ($0 < N < 96$), where $N = 96$ corresponds to 263 mg H_2O/g clay for uranyl-montmorillonite or 300 mg H_2O/g clay for Ca-montmorillonite. The well-known positive correlation between layer spacing (c_z) and water content (Boek *et al.*, 1995; Young and Smith, 2000) is seen in Figure 1. Standard deviations in the c_z values range from 0.07 Å ($N = 0$) to 0.15 Å ($N = 62$ and $N = 96$). As more water

molecules are forced into the system, the layer spacing increases to accommodate them while maintaining equilibrium. We see no strong evidence for plateau regions characteristic of one- and two-layer hydrates, as with some monatomic counterions (Boek *et al.*, 1995; Young and Smith, 2000), including the Ca-montmorillonite data shown for comparison. The larger error bars (0.12–0.14 Å) in layer spacing at low water content ($27 < N < 39$) indicate that the system was especially unstable at these state points. For $N = 27$, 33 and 39, simulations were initiated by removing three water molecules from equilibrium configurations of the $N = 30$, 36 and 42 systems, respectively. We chose only water molecules that were not coordinated to uranyl cations. These 'desorption' simulations resulted in average layer spacing values that were ~0.5 Å less than the values obtained from a random start. Average interlayer potential energies were also lower in the 'desorption' simulations. This effect could be signs of hysteresis in clay swelling (Boek *et al.*, 1995; Young and Smith, 2000) or an issue of inadequate phase space sampling in the MC algorithm. However, we are mainly interested in state points in which the layer spacing is in the range of 14.5–15.0 Å, which have been reported from X-ray diffraction (XRD) measurements of hydrated UO_2^{2+}-montmorillonite (Tsunashima *et al.*, 1981; Dent *et al.*, 1992). Three points ($N = 58$, 62, 64) fit this description, and we used the $N = 58$ case for detailed comparison with EXAFS data and for MD simulations.

Uranyl atomic density profiles, which show relative atomic density as a function of vertical position (z), are shown in Figure 2 as a function of water content. For the
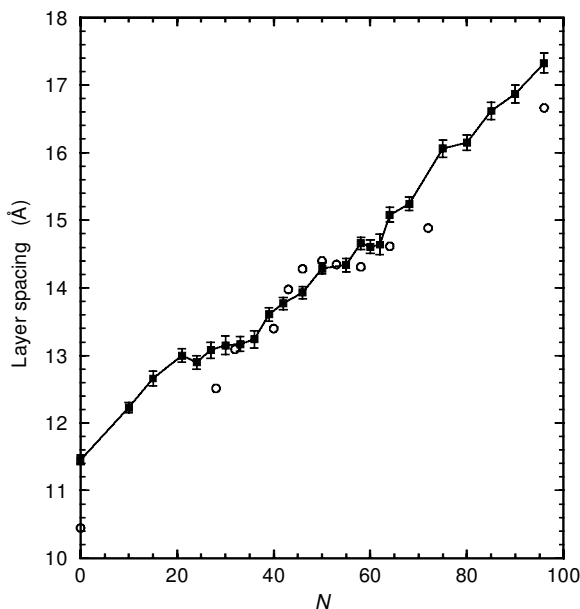

Figure 1. Simulated swelling curve for uranyl-montmorillonite (filled squares). Average layer spacing and standard deviation are shown for each value of N. Results for Ca-montmorillonite (open circles) (Greathouse and Storm, 2002) are shown for comparison.
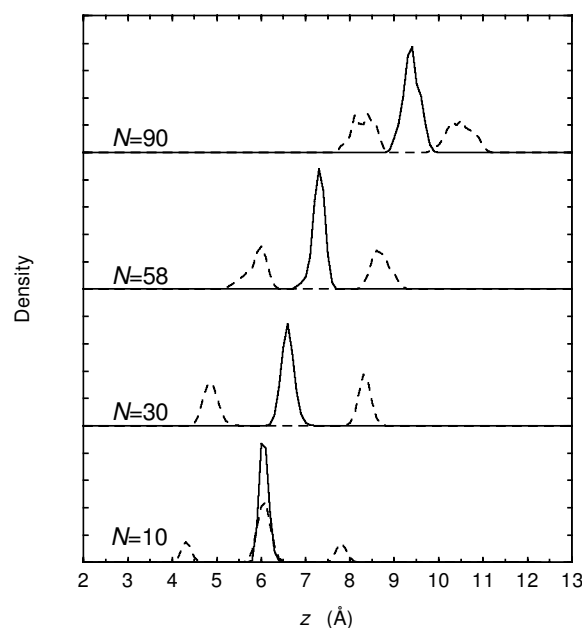

Figure 2. Uranyl U (solid line) and oxygen (dashed line) density profiles from MC simulations. Water content is indicated next to each curve.

Table 2. Average RDF peak distances and coordination numbers from Figure 3.

Water content (N)	c_z (Å)	Shell	Peak max (Å)	Peak min (Å)	Coordination number[a]
10	12.23	U−O$_{eq}$	2.35	2.70	3.15
		U−Si	3.55	3.85	1.86
		U−O	3.65	4.65	10.97
30	13.15	U−O$_{eq}$	2.45	2.90	5.00
		U−Si	4.80	5.90	11.99
		U−O	4.20	4.95	16.07
58	14.66	U−O$_{eq}$	2.45	2.90	5.00
		U−Si	5.10	5.55	5.00
		U−O	4.45	5.50	19.87
90	16.87	U−O$_{eq}$	2.45	2.90	5.00
		U−Si	4.85	5.20	1.05
		U−O	4.75	5.60	21.48

[a] Coordination numbers were determined by integrating the RDF up to the minimum value of each peak. Second-shell U−O coordination numbers include oxygen atoms in both the first and second shells.

N = 58 system, the U atoms are most likely to be found at z = 7.3 Å. The uranyl cation is always centered at the midplane, with one oxygen atom each above and below the midplane. As N (and layer spacing) increases, the atomic density peaks shift to higher values. At each water content, the distance between U and O peak centers is slightly less than 1.8 Å (the fixed U−O bond length), which indicates that the ions are tilted slightly from the surface normal. The N =10 system is characterized by a different density profile. With insufficient water molecules needed for five-fold coordination to three uranyl cations, one uranyl cation orients itself perpendicular to the surface normal and coordinates to surface oxygen atoms. For this cation, U and O atoms have the same z coordinate. At much higher water content (N = 90 in Figure 2), the UO$_2$(H$_2$O)$_5^{2+}$ complexes have much more rotational freedom, resulting in the broader U and O density peaks.

Averaged RDF data are shown in Table 2 and Figure 3. At every water content, the first peaks in the U−O radial distribution functions have nearly identical structure. A depletion zone in U−O graphs between 2.9 Å and 3.4 Å separates the first- and second-shell oxygen atoms. The RDF results also suggest that the molecular composition of the first shell about uranyl cations is consistent at low and high water contents. The first U−O peak at 2.45 Å agrees well with the values of 2.41 Å and 2.43 Å seen from EXAFS experiments (Giaquinta *et al.*, 1997; Sylwester *et al.*, 2000). The one exception is at very low water content (N = 10), which is identified by the poorly defined depletion zone and a lower U−O coordination number in the first shell (Table 2). As N increases, the second oxygen shell (beginning at 3.4 Å) becomes broader due to water exchange. Looking at the U−Si peaks (dashed lines in Figure 3), we see further evidence for the uranyl orientation discussed above. For the N = 30 and higher states, Si atoms in the clay layer are never closer than 4.0 Å to the U atom, which precludes the existence of an inner-sphere complex. It is also interesting to note that

the U−Si coordination number decreases as N increases, which implies that the uranyl ions are gradually moving farther from the surfaces. The inner-sphere complex seen in the N = 10 system results in the U−Si peak at 3.55 Å.

Equilibrium snapshots for N = 58 are shown in Figure 4. The upper clay layer has shifted significantly in the x direction as a direct result of registration. The average **c** vector components from the MC simulation were c_x = 4.36±0.25 Å, c_y = 1.32±0.42 Å, c_z = 14.66±0.09 Å. We see two distinct water layers, with water molecules oriented to form hydrogen bonds with the nearest siloxane surface (Figure 4a). Water molecules near the midplane usually occupy a uranyl coordination shell. Looking in the (x,y) plane (Figure 4b), the first-shell coordination geometry about
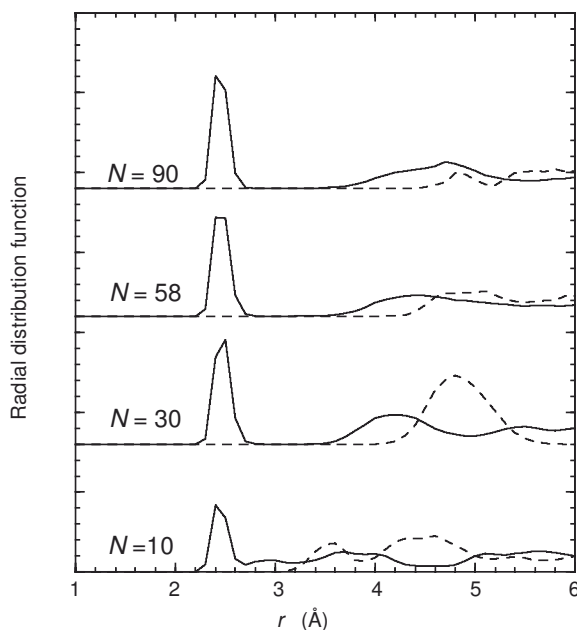

Figure 3. Radial distribution functions from MC simulations for U−O (solid line) and U−Si (dashed line) correlations. Water content is indicated next to each curve.
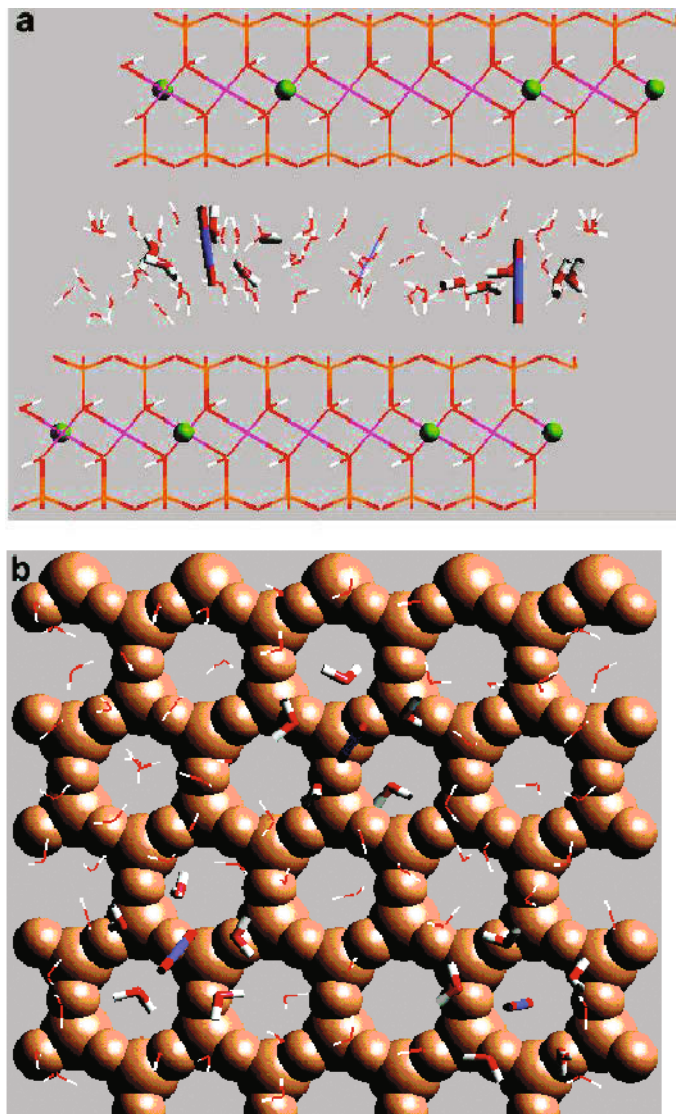
Figure 4. Equilibrium MC snapshots for $N = 58$. (a) View in the (x,z) plane with atoms colored as follows: U (blue), O (red), H (white), Si (orange), Al (magenta), Mg (green). Two uranyl cations and their first-shell water molecules are shown as tubes, while all other interlayer atoms are shown as sticks. Charge sites in the clay octahedral sheet (Mg^{2+} ions) are shown as spheres. (b) View in the (x,y) plane with interlayer atoms colored as in (a). Clay atoms comprising the lower siloxane surface are shown as brown spheres for clarity.

the U atoms is visible, with water oxygen atoms occupying equatorial positions and uranyl O atoms in axial positions. We can clearly discern the orientation of uranyl cations with respect to the surface normal. Interestingly, the rightmost uranyl ion is oriented nearly parallel to the surface normal, with one oxygen atom keyed into the lower ditrigonal cavity. The z coordinate for this U atom is below the midplane to facilitate interactions between the lower uranyl oxygen atom and the surface (Figure 4a). In analyzing their EXAFS results, Giaquinta *et al.* (1997) reported a small second peak in the U–O distribution at a distance of 3.45 Å and a coordination number of 2.6. The rightmost uranyl

shown in Figure 4b best illustrates the model used to explain this result, with surface oxygen atoms comprising the second peak (Giaquinta *et al.*, 1997). The rightmost uranyl cation in Figure 4b is usually off center with respect to the ditrigonal cavity. As a result, that U atom is between 3.5 Å and 4.0 Å from the three nearest surface oxygen atoms in the cavity and farther than that from the other three oxygen atoms. Thus a second U–O shell should only contain 2 or 3 oxygen atoms, in agreement with experiment (Giaquinta *et al.*, 1997). However, we cannot discern such a small peak from the broader U–O second shell peaks in our RDF results (Figure 3).

For the two-layer hydrate, Figures 1–3 reveal that no uranyl ions are oriented perpendicular to the surface normal at equilibrium. In order to determine if the uranyl orientation we see is truly the lowest energy configuration, we began a new set of simulations with one or more uranyl cations oriented perpendicular to the surface normal. The U atoms were placed within 3.0 Å from the surface to facilitate the formation of an inner-sphere complex. At equilibrium, however, only the uranyl orientations shown in Figure 4 were seen (outer-sphere complex), indicating that the perpendicular orientation (inner-sphere complex) results in a higher potential energy.

Recent XAS experiments have yielded a consistent picture of the interlayer structure of uranyl-smectites: a single equatorial shell of oxygen atoms with an average U–O distance of ~2.4 Å, suggesting an outer-sphere complex (Dent *et al.*, 1992; Giaquinta *et al.*, 1997; Denecke *et al.*, 1999; Sylwester *et al.*, 2000). Qualitatively, our structural results compare well with these data. Further, we are confident that our 58-water model system represents a comparable hydration state because our average layer spacing (14.7 Å) is in good agreement with the experimental value of 14.8 Å reported by Giaquinta *et al.* (1997). An additional factor that we must consider when comparing simulation results with experiment is the specific smectite used. Sylwester *et al.* (2000) used SAz-1, which, like our model, contains negative charge exclusively in the octahedral sheet. Other studies used clays with a small fraction of tetrahedral sheet charge (Dent *et al.*, 1992; Giaquinta *et al.*, 1997; Denecke *et al.*, 1999). The presence of tetrahedral charge sites, with negative charge much closer to the siloxane surface, could lead to inner-sphere uranyl complexes. We are currently investigating this problem.

Dynamic properties

We used MD simulations to investigate the time evolution of interlayer properties in equilibrated UO_2^{2+}-montmorillonite hydrates. We present results for the two-layer hydrate ($N = 58$) only, as the corresponding layer spacing best compares with experimental values. Interlayer molecules (water and uranyl) are labeled 0–60 so that each molecule can be separately recognized. In Figure 5, we see a consistent orientation for the three uranyl ions throughout the 1.0 ns simulation. This orientation could best be described as slightly bent from the surface normal, at an angle of ~30°. This angle is often well below 30° in certain long periods (up to 0.3 ns, Uranyl 60 in Figure 5), indicating that the ions occasionally assume a more parallel orientation. With only three cations in the simulation, time-averaged values for uranyl orientation or residence times cannot be predicted with statistical reliability. We note that the angle never surpasses 60°, which indicates that the uranyl cations are never oriented perpendicular to the surface normal.

The mobility of uranyl cations and water molecules can be visualized by plotting center-of-mass trajectories in either the (x,y) or (x,z) plane. We present (x,y) trajectories only because the uranyl ions remained at or near the midplane throughout the MD simulation (data not shown). Looking at the uranyl trajectories (Figure 6), we see that two ions are quite mobile, while the third maintains a stationary complex with the surface. For Uranyl 59 and Uranyl 60, the translational motion is best described as jump diffusion events (Poinsignon *et al.*, 1987; Axe and Anderson, 1998) followed by periods of limited mobility at a fixed
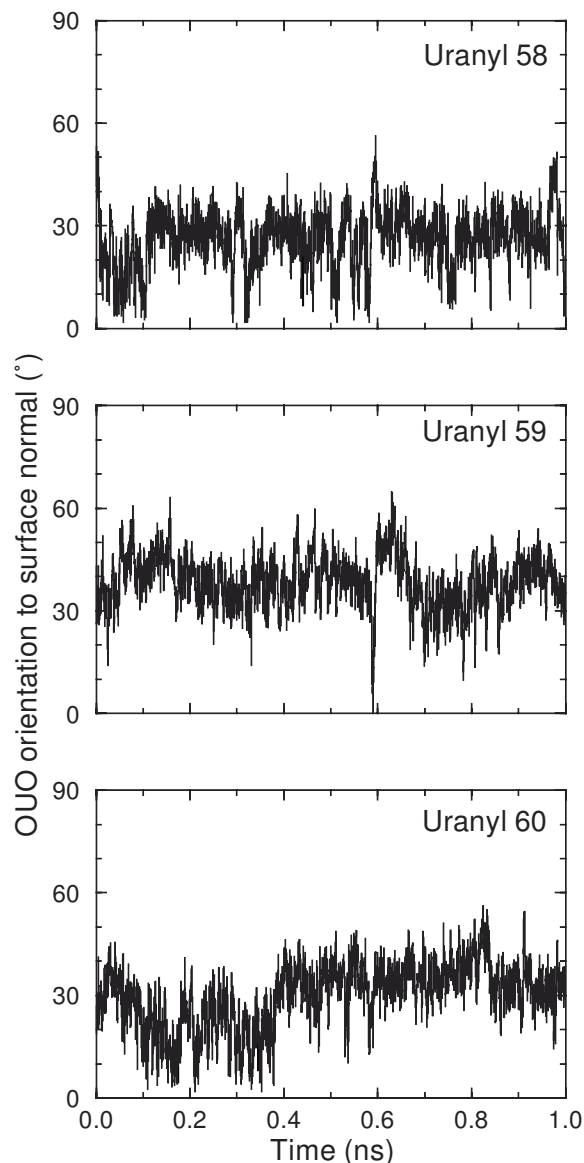

Figure 5. Time evolution of uranyl orientation for MD simulation. Each graph plots the O–U–O vector orientation with respect to the surface normal for each ion. A value of 0° indicates that the O–U–O is parallel to the surface normal, while a value of 90° indicates perpendicular orientation.
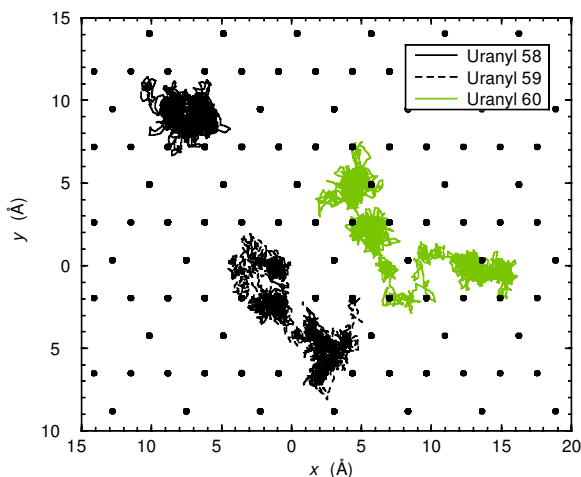
Figure 6. MD trajectories for uranyl cations (strictly U atoms). Each connected point represents the position of that molecule every 0.05 ps. Small black circles indicate the location of oxygen atoms on the lower siloxane surface.
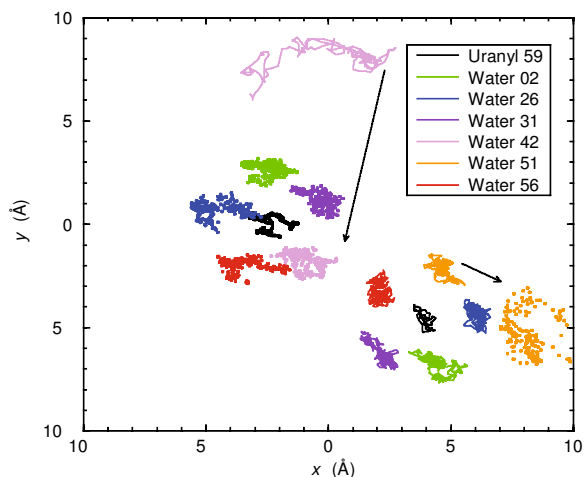

Figure 7. MD trajectories for one uranyl cation and six water molecules. Trajectories shown as lines occur early in the simulation (0–10 ps), while trajectories shown as dots occur later in the simulation (600–610 ps). Arrows highlight two water molecules involved in an exchange event between the two time periods.

location. As these cations traverse the surface, U atoms move above and below the midplane as the cations are briefly keyed into ditrigonal cavities.

We can also track the movement of water molecules within the $UO_2(H_2O)_5^{2+}$ complexes. These coordinating water molecules are exchangeable and interchangeable. That is, they are exchangeable with non-coordinating water molecules, and they are interchangeable within the first shell. As Figure 7 shows, Water 51 is part of the first shell at an initial stage of the simulation (lower right), but it is eventually replaced by Water 42 (center). Additionally, Water 56 changes its position in the first shell relative to the other water molecules. This exchange probably occurred during a jump diffusion event of the entire $UO_2(H_2O)_5^{2+}$ complex. In any case, Figure 7 demonstrates that the first U–O shell is not fixed and the identity of first-shell water molecules is not fixed, and neither are their relative positions within the shell. The results shown here for a single uranyl coordination shell are consistent with all three cations in the simulation.

CONCLUSIONS

We have presented results for computer simulations of aqueous uranyl cations near clay surfaces based on published potential parameters. Our smectite model consists of a montmorillonite clay with negative charge exclusively in the octahedral sheet facilitating comparison with experimental data and avoiding simulation difficulties with tetrahedral substitution. Our MC results reveal a consistent interlayer structure, with uranyl cations oriented nearly parallel to the surface normal in an outer-sphere complex. The first coordination shell consists of five water molecules located in the equatorial

plane, although there is exchange of water molecules over the 1 ns time scale of our MD simulations. Occasionally (but not always) uranyl cations are keyed into ditrigonal cavities on the siloxane surface. The high degree of uranyl mobility suggests that a uranyl cation keyed into a ditrigonal cavity does not stabilize the system enough to prevent further cation diffusion. We have not attempted to analyze the hydrogen bonding network within the interlayer, other than to point out those that exist between water molecules and the siloxane surface. A systematic study of interlayer hydrogen bonding as a function of water content could help to explain why we did not see a well-developed plateau region in Figure 1.

Another possibility for interlayer uranyl structure consists of inner-sphere complexes with the cations oriented perpendicular to the surface normal (Sylwester *et al.*, 2000). Our MC simulations showed that such inner-sphere complexes resulted in a higher potential energy and were never seen at equilibrium. However, when the smectite bears negative charge in the tetrahedral sheet, uranyl cations may in fact form inner-sphere complexes. With the layer charge so close to the clay surface, the strong Coulombic attraction between the negative charge site and the positive U atom may cause a reorientation of the uranyl cation, with surface oxygen atoms taking positions in the first coordination shell. However, we require a more reliable model for tetrahedrally substituted clays to investigate this possibility properly.

ACKNOWLEDGMENTS

REFERENCES

Allen, M.P. and Tildesley, D.J. (1987) *Computer Simulation of Liquids.* Clarendon Press, Oxford, UK, 385 pp.

Axe, L. and Anderson, P.R. (1998) Intraparticle diffusion of metal contaminants in amorphous oxide minerals. Pp. 193–208 in: *Adsorption of Metals by Geomedia* (E.A. Jenne, editor). Academic Press, San Diego, USA.

Berendsen, H.J.C., Grigera, J.R. and Straatsma, T.P. (1987) The missing term in effective pair potentials. *Journal of Physical Chemistry*, **91**, 6269–6271.

Boek, E.S., Coveney, P.V. and Skipper, N.T. (1995) Monte Carlo molecular modeling studies of hydrated Li-, Na-, and K-smectites: Understanding the role of potassium as a clay swelling inhibitor. *Journal of the American Chemical Society*, **117**, 12608–12617.

Breen, C., Madejová, J. and Komadel, P. (1995) Characterisation of moderately acid-treated, size-fractionated montmorillonites using IR and MAS NMR spectroscopy and thermal analysis. *Journal of Materials Chemistry*, **5**, 469–474.

Chang, F.-R.C., Skipper, N.T. and Sposito, G. (1995) Computer simulation of interlayer molecular structure in sodium montmorillonite hydrates. *Langmuir*, **11**, 2734–2741.

Chang, F.-R.C., Skipper, N.T. and Sposito, G. (1997) Monte Carlo and molecular dynamics simulations of interfacial structure in lithium-montmorillonite hydrates. *Langmuir*, **13**, 2074–2082.

Chang, F.-R.C., Skipper, N.T. and Sposito, G. (1998) Monte Carlo and molecular dynamics simulations of electrical double-layer structure in potassium-montmorillonite hydrates. *Langmuir*, **14**, 1201–1207.

Chavez-Paez, M., dePablo, L. and dePablo, J.J. (2001) Monte Carlo simulations of Ca-montmorillonite hydrates. *Journal of Chemical Physics*, **114**, 10948–10953.

Chisholm-Brause, C.J., Berg, J.M., Matzner, R.A. and Morris, D.E. (2001) Uranium (VI) sorption complexes on montmorillonite as a function of solution chemistry. *Journal of Colloid and Interface Science*, **233**, 38–49.

Denecke, M.A., Bauer, A., Kim, J.I. and Moll, H. (1999) Polarization dependent XANES of uranium(VI) sorbed onto smectite. Pp. 35–37 in: *Mineral/Water Interactions Close to Equilibrium* (W. Schussler and A. Bauer, editors). Workshop, Speyer, March 25–26, 1999, Forschungszentrum Karlsruhe GmbH, Karlsruhe, Germany.

Dent, A.J., Ramsay, J.D.F. and Swanton, S.W. (1992) An EXAFS study of uranyl ion in solution and sorbed onto silica and montmorillonite clay colloids. *Journal of Colloid and Interface Science*, **150**, 45–60.

Floris, F.M., Perisco, M., Tani, A. and Tomasi, J. (1994) Hydration shell structure of the calcium ion from simulations with ab initio effective pair potentials. *Chemical Physics Letters*, **227**, 126–132.

Giaquinta, D.M., Soderholm, L., Yuchs, S.E. and Wasserman, S.R. (1997) The speciation of uranium in a smectite clay: Evidence for catalysed uranyl reduction. *Radiochimica*

Acta, **76**, 113–121.

Grauer, R. (1994) Bentonite as a backfill material in a high-level waste repository. *MRS Bulletin*, **19**, 43–46.

Greathouse, J.A. and Storm, E.W. (2002) Calcium hydration on montmorillonite clay surfaces studied by Monte Carlo simulation. *Molecular Simulation*, **28**, 633–647.

Greathouse, J.A., Refson, K. and Sposito, G. (2000) Molecular dynamics simulation of water mobility in magnesium-smectite hydrates. *Journal of the American Chemical Society*, **122**, 11459–11464.

Greathouse, J.A., O'Brien, R.J., Bemis, G. and Pabalan, R.T. (2002) Molecular dynamics study of aqueous uranyl interactions with quartz (010). *Journal of Physical Chemistry B*, **106**, 1646–1655.

Guilbaud, P. and Wipff, G. (1996) Force field representation of the UO_2^{2+} cation from free energy MD simulations in water. Tests on its 18-crown-6 and NO_3 adducts, and on its calix[6]arene[6-] and CMPO complexes. *Journal of Molecular Structure (THEOCHEM)*, **366**, 55–63.

Hartzell, C.J., Cygan, R.T. and Nagy, K.L. (1998) Molecular modeling of the tributyl phosphate complex of europium nitrate in the clay hectorite. *Journal of Physical Chemistry A*, **102**, 6722–6729.

Hyun, S.P., Cho, Y.H., Hahn, P.S. and Kim, S.J. (2001) Sorption mechanism of U(VI) on a reference montmorillonite: binding to the internal and external surfaces. *Journal of Radioanalytical and Nuclear Chemistry*, **250**, 55–62.

Lajudie, A., Raynal, J., Petit, J.-C. and Toulhoat, P. (1994) Clay-based materials for engineered barriers: A review. Pp. 221–231 in: *Scientific Basis for Nuclear Waste Management XVIII* (T. Murakami and R.C. Ewing, editors). Materials Research Society, Pittsburgh, Pennsylvania, USA.

McKinley, J.P., Zachara, J.M., Smith, S.C. and Turner, G.D. (1995) The influence of uranyl hydrolysis and multiple site-binding reactions on adsorption of U(VI) to montmorillonite. *Clays and Clay Minerals*, **45**, 586–598.

National Research Council (2000) *Research needs in Subsurface Science.* National Academy Press, Washington, D.C.

Neall, F.B., Baertschi, P., McKinley, I.G., Smith, P.A., Sumerling, T. and Umeki, H. (1995) Comparison of the concepts and assumptions in five recent HLW/spent fuel performance assessments. Pp. 503–510 in: *Scientific Basis for Nuclear Waste Management XVIII* (T. Murakami and R.C. Ewing, editors). Materials Research Society, Pittsburgh, Pennsylvania, USA.

Pabalan, R.T. and Turner, D.R. (1997) Uranium (6+) sorption on montmorillonite: experimental and surface complexation modeling study. *Aquatic Geochemistry*, **2**, 203–226.

Pabalan, R.T., Turner, D.R., Bertetti, F.P. and Prikryl, J.D. (1998) Uranium(VI) sorption onto selected mineral surfaces. Pp. 99–130 in: *Adsorption of Metals by Geomedia* (E. Jenne, editor). Academic Press, San Diego, California.

Poinsignon, C., Estrade-Szwarckopf, J., Conard, J. and Dianoux, A.J. (1987) Water dynamics in the clay-water system: A quasi-elastic neutron scattering study. Pp. 284–291 in: *Proceedings of the International Clay Conference Denver* (L.G. Schultz, H. van Olphen and F.A. Mumpton, editors). Clay Minerals Society, Bloomington, Indiana.

Reeder, R.J., Nugent, M. and Pabalan, R.T. (2001) Local structure of uranium (VI) sorbed on clinoptilolite and montmorillonite. Pp. 423–426 in: *Water-Rock Interaction* (R. Cidu, editor). A.A. Balkema, Lisse, The Netherlands.

Refson, K. (2000) Moldy: a portable molecular dynamics simulation program for serial and parallel computers. *Computer Physics Communications*, **126**, 310–329.

Riley, R.G., Zachara, J.M. and Wobber, F.J. (1992) *Chemical Contaminants on DOE Lands and Selection of Contaminant*

Mixtures for Subsurface Science Research. US Department of Energy, Office of Energy Research, Washington, D.C.

Skipper, N.T. (1996) *MONTE User's Manual.* Department of Physics and Astronomy, University College, London.

Skipper, N.T., Refson, K. and McConnell, J.D.C. (1991) Computer simulation of interlayer water in 2:1 clays. *Journal of Chemical Physics*, **94**, 7434–7445.

Skipper, N.T., Chang, F.-R.C. and Sposito, G. (1995) Monte Carlo simulation of interlayer molecular structure in swelling clay minerals. 1. Methodology. *Clays and Clay Minerals*, **43**, 285–293.

Smith, D.E. (1998) Molecular computer simulations of the swelling properties and interlayer structure of cesium montmorillonite. *Langmuir*, **14**, 5959–5967.

Sylwester, E.R., Hudson, E.A. and Allen, P.G. (2000) The structure of uranium (VI) sorption complexes on silica, alumina, and montmorillonite. *Geochimica et Cosmochimica Acta*, **64**, 2431–2438.

Teppen, B.J., Rasmussen, K.R., Bertsch, P.M., Miller, D.M. and Schafer, L. (1997) Molecular dynamics modeling of clay minerals. 1. Gibbsite, kaolinite, pyrophillite, and beidellite. *Journal of Physical Chemistry B*, **101**, 1579–1587.

Teppen, B.J., Yu, C.-H., Miller, D.M. and Schafer, L. (1998) Molecular dynamics simulations of sorption of organic compounds at the clay mineral/aqueous solution interface. *Journal of Computational Chemistry*, **19**, 144–153.

Tsunashima, A., Brindley, G.W. and Bastovanov, M. (1981) Adsorption of uranium from solutions by montmorillonite: compositions and properties of uranyl montmorillonites. *Clays and Clay Minerals*, **29**, 10–16.

Young, D.A. and Smith, D.E. (2000) Simulations of clay mineral swelling and hydration: dependence upon interlayer ion size and charge. *Journal of Physical Chemistry B*, **104**, 9163–9170.

Zachara, J.M. and McKinley, J.P. (1993) Influence of hydrolysis on the sorption of metal cations by smectites: Importance of edge coordination reactions. *Aquatic Science*, **55**, 251–261.